Water Research 170 (2020) 115354

Contents lists available at ScienceDirect

Water Research

journal homepage: www.elsevier.com/locate/watres

Ecotoxicological effects of sulfonamide on and its removal by the submerged plant *Vallisneria natans* (Lour.) Hara

Liming Zhu [a, 1], Houtao Xu [b, 1], Wensheng Xiao [a], Jianke Lu [a], Di Lu [a], Xiaoyu Chen [a], Xiaoyan Zheng [c], Erik Jeppesen [d, e, f], Wei Zhang [a, *], Liqing Wang [a, **]

[a] Centre for Research on Environmental Ecology and Fish Nutrient of the Ministry of Agriculture, Key Laboratory of Exploration and Utilization of Aquatic Genetic Resources of the Ministry of Education, National Demonstration Center for Experimental Fisheries Science Education, Shanghai Ocean University, Shanghai, 201306, PR China
[b] School of Agriculture and Biology, Shanghai Jiao Tong University, 800 Dongchuan Road, Shanghai, 200240, PR China
[c] Shanghai Aquatic Environmental Engineering Co., Ltd, Shanghai, 201306, PR China
[d] Department of Bioscience, Aarhus University, Silkeborg, 8600, Denmark
[e] Sino-Danish Centre for Education and Research (SDC), University of Chinese Academy of Sciences, Beijing, 100049, PR China
[f] Limnology Laboratory and EKOSAM, Department of Biological Sciences, Middle East Technical University, Ankara, Turkey

ARTICLE INFO

Article history:
Received 3 August 2019
Received in revised form
27 November 2019
Accepted 28 November 2019
Available online 30 November 2019

Keywords:
Sulfonamide
Vallisneria natans
Ecotoxicological effects
Removal mechanism
Microbial community

ABSTRACT

The extensive application of sulfonamides (SAs) raises concern regarding its negative environmental effects. In aquatic environments, macrophytes may not only be affected by various pollutants, they may also help to reduce the concentrations in the surrounding environment. We studied both the ecotoxicological effects of sulfonamide (SN) on and its removal by *Vallisneria natans* (Lour.) Hara, an important submerged macrophyte in Chinese lakes and rivers. The toxic effect and oxidative stress caused by SN resulted in a reduction of total chlorophyll (chl.a and b) and autofluorescence of chloroplast. Meanwhile, the levels of reactive oxygen species (ROS, including O_2^- and H_2O_2) and peroxidase (POD) increased with increasing SN concentration and duration of exposure. After 20 days' exposure, a reduction in the relative growth rate (RGR) and leaf length of *V. natans* was found under SN stress, but SN had only a weak effect on root length. Although high SN concentrations had toxic effects on the growth of *V. natans*, the plant was overall resistant to the SN doses that we used. We studied the effect of *V. natans* on sulfonamide removal in an additional 13-day exposure experiment with focus on the dynamics of dissolved oxygen (DO), the oxidation-reduction potential (ORP) and microbial communities in the water column, as well as in the periphyton on *V. natans* surfaces. The results show that presence of *V. natans* significantly improved the SN removal efficiency likely by increasing DO, ORP and bacterial diversity in the water column. The presence of *V. natans* led to higher relative abundances of *Saccharimonadales* and *Rhizoniales*. Lefse analysis showed that *Saccharimonadales*, *Micrococcales*, *Sphingobacteriales*, *Bacteroidales*, *Obscuribacterales*, *Flavobacteriales*, *Pseudomonadaceae* and *Myxococcales*, which are considered to be SN-resistant bacteria, increased significantly in the V + S+ (*V. natans* and SN) treatment compared with the V + S- (*V. natans* and no SN) treatment and V−S+ (no *V. natans* and SN) treatment. As far as we know, ours is the first study of the ecotoxicological effects of sulfonamide and its removal by submerged vascular plants (here *V. natans*). Thus, our results add to the understanding of the antibiotic removal mechanism of macrophytes in freshwater systems and help to clarify the linkages between antibiotics and macrophyte-microbe systems; thereby providing new insight into ecological-based removal of antibiotics in aquatic systems.

* Corresponding author. College of Fisheries and Life Science, Shanghai Ocean University, Shanghai, 201306, China.
** Corresponding author.College of Fisheries and Life Science, Shanghai Ocean University, Shanghai, 201306, China.
E-mail addresses: weizhang@shou.edu.cn (W. Zhang), lqwang@shou.edu.cn (L. Wang).
[1] These authors contributed equally to this work.

https://doi.org/10.1016/j.watres.2019.115354
0043-1354/

1. Introduction

Sulfonamides (SAs) have been used for more than 50 years within the fields of veterinary chemotherapeutics and human medicine due to their low cost and broad spectrum of activity in preventing or treating bacterial infections (Białk-Bielińska et al., 2011). However, SAs are poorly absorbed in the gut and not completely metabolised by higher organisms, and they are usually excreted as the parent compounds or metabolites (García-Galán et al., 2008). In addition, due to the incomplete removal during wastewater treatment and their continued release into the environment, SAs are frequently detected in the aquatic environment (Kümmerer, 2009). Take China as an example: The consumption and production of antibiotics in China are the highest in the world (Li et al., 2018). SAs in water samples collected from feedlot wastewater pools and irrigation ditches in Shanghai City have shown total concentrations of 198–323 μg L^{-1} (Ji et al., 2011), and in the Yangtze Estuary and Huangpu River SAs concentrations up to 219 ng L^{-1} and 313 ng L^{-1} have been recorded (Yan et al., 2013). Although the average concentrations of SAs in environmental samples are low (at the μg L^{-1} or ng L^{-1} level) (Li et al., 2018), they are continuously being released, so they will eventually pose a serious environmental risk (García-Galán et al., 2009; Santos et al., 2010).

SAs are designed to target specific metabolic pathways (they competitively inhibit the conversion of p-aminobenzoic acid, pABA) by inhibiting the biosynthetic pathway of folate (an essential molecule required by all living organisms), so they not only affect bacteria but may also, to a varying degree, have unwanted effects on other organisms, such as microalgae, zooplankton, fish and macrophytes (García-Galán et al., 2009; Park and Choi, 2008; Schauss et al., 2009). In general, removal of SAs is achieved through activated sludge (based on microorganisms and adsorption) (Yang et al., 2012, 2016), ozonation (based on oxidation) (García-Galán et al., 2012) and magnetic nanocomposite (based on adsorption) (Bao et al., 2013). However, so far, only few studies have focused on antibiotic phytoremediation in natural aquatic ecosystems, although uptake by crop plants of antibiotics has been extensively reported (Eggen et al., 2011; Migliore et al., 2003).

Phytoremediation is a new technology that uses plants to degrade, assimilate, metabolise or detoxify metals (Kamal et al., 2004), hydrocarbons (Wang, 2004), pesticides (Gao et al., 2000) and chlorinated solvents (Roy et al., 1994). Aquatic macrophytes play the key role in removing pollutants, improving water quality and maintaining aquatic ecosystem stability (Wang et al., 2011). Several studies have clarified the removal process of nutrients and conventional organic pollutants by submerged plants through absorption (Zhu et al., 2016a, 2016b). However, knowledge about the removal of antibiotics by submerged macrophytes, especially by changing the surrounding physical and chemical environment and thereby shaping the microbial community in the water column and the epiphytic biofilm, is still fragmentary.

Vallisneria natans (Lour.) Hara is a fully submerged, perennial, rooted plant and is widely distributed in freshwaters in China (Wang et al., 2011) where it plays an important role in maintaining the health of aquatic ecosystems by releasing oxygen and providing food and shelter for aquatic animals (Rai et al., 1995). Moreover, it can also assimilate toxic components and thereby reduce their concentrations in the surrounding water. *V. natans* has been shown to take up microcystin-RR (Yin et al., 2005), heavy metals (Chen et al., 2014) and other organic pollutants (including pesticides, pharmaceuticals and personal care products) (Gao et al., 2000; Olette et al., 2008). Now, *V. natans* has become one of the most important aquatic plants in China for evaluating aquatic environmental pollution and ecological restoration (Wang et al., 2011). However, hitherto, the effects of emerging pollutants (ex: antibiotic pollutants) on and their removal by *V. natans* remain poorly elucidated.

The main objectives of the present study were to: (1) explore the tolerance of *V. natans* to high concentration of sulfonamide (SN) through the physiological and morphologic response of *V. natans* to SN exposure; (2) explore whether the presence of *V. natans* can enhance the removal efficiency of SN in the water column. We hypothesised that *V. natans* would overall be resistant to natural SN doses and that its presence could enhance the removal of SN by changing the redox environment of the water body and by altering the microbial communities of the water column. We investigated ecotoxicological effects of SN and its removal by *V. natans* for the first time. Our results might add to the understanding of the antibiotic removal mechanism of macrophytes in freshwater systems and help to clarify the linkages between antibiotics and macrophyte-microbe systems. Our study provides new insight into ecological removal of antibiotics in lakes and rivers in China.

2. Materials and methods

2.1. Chemicals

SN (>99.8% purity) and other chemicals were purchased from Sinopharm Chemical Reagent Co., Ltd (China), and the physicochemical properties of SN are presented in Table S1. The chemical contents of Hoagland solution are given in Table S2 (Xue and Yan, 2011).

2.2. V. natans incubation and treatments

V. natans plants were collected from a small freshwater lake, Lake Minghu (30°53′14″N, 121°53′23″E), located in the campus of Shanghai Ocean University, Shanghai, China, where the species dominates the macrophyte community. Before exposure to SN, the plants were acclimatised for two weeks under laboratory conditions (10% Hoagland solution, constant white light on a 12:12 L/D cycle, 25 ± 1 °C). After two weeks of pre-incubation, we selected approx. 5 -cm long *V. natans* seedlings with three leaves and no branches for the experiments.

2.3. Experimental design

2.3.1. Ecotoxicology experiment

In order to observe the toxicological response and tolerance of *V. natans* to high concentrations of SN, thirty approximately similar *V. natans* seedlings (total fresh weight: 71.58 ± 2.44 g, mean ± SD; average length: ~5 cm) were collected and transferred to a tank (Fig. S1) containing glass beads and 10% Hoagland solution with four levels of SN (0, 10, 30 and 50 mg L^{-1}); there were four replicates of each SN level. All culture solutions were refreshed in a static way every 5 days throughout the acclimation and experimental periods. All tanks were incubated as described in Section 2.2. During the experiment, we randomly collected one *V. natans* seedling from each tank on day 0 and day 20, respectively. The periphyton attached to the plant leaves and roots was removed using a soft brush. The leaves and roots were washed with distilled water and dried carefully with blotting paper, after which the fresh weight of the plant (FW) was measured and the relative growth rate (RGR) calculated. After 0, 10 and 20 days of exposure, one *V. natans* seedling was collected randomly from each tank to measure leaf length and root length. The leaves of the seedlings were frozen in an ice bath to measure total chlorophyll, chlorophyll *a* (Chl.a), chlorophyll *b* (Chl.b), malondialdehyde (MDA), O_2^-, H_2O_2 and peroxidase (POD) activity. After 20 days of exposure, fresh leaf

tissue of *V. natans* from the different levels of the SN treatments was collected randomly to measure chloroplast autofluorescence.

2.3.2. Removal of SN by V. natans

The removal of SN was studied in tanks (Fig. S1). Three treatment groups were assigned: V + S- (*V. natans* and no SN), V−S+ (no *V. natans* and SN), V + S+ (*V. natans* and SN). All treatments were run with four replicates and the experiment lasted for 13 days. Several previous studies on removal of antibiotics have used high concentrations (10 mg L^{-1} to 100 mg L^{-1}) (Xiong et al., 2017; Li et al., 2015), and by applying concentrations higher than the typical natural SN concentrations (30 mg L^{-1}), we expected to more easily detect the effect of *V. natans* on the maintenance of the microbial community and the removal of antibiotics. In the beginning of the experiment, the SN concentration was measured every second day, and dissolved oxygen (DO) and the oxidation-reduction potential (ORP) were recorded every day. Microbial samples from the water and the leaf surface were collected on day 11, including five types: WV + S- (Water sample, *V. natans* and no SN), WV-S+ (Water sample, no *V. natans* and SN), WV + S+ (Water sample, *V. natans* and SN), PV + S- (Periphyton sample, *V. natans* and no SN), PV + S+ (Periphyton sample, *V. natans* and SN). All fresh samples were stored in liquid nitrogen and then frozen at - 80 °C until the extraction of DNA.

2.4. Relative growth rate

The relative growth rate (RGR) is calculated according to the following formula:

$$\mathrm{RGR}\ (\%) = \frac{W - W0}{W0} \times 100\%$$

where W_0 is the fresh weight of the plant at the initial incubation time (day 0), and W is the fresh weight at the end of the experiment (day 20).

2.5. Determination of chlorophyll and autofluorescence of chloroplast in plant leaves

Chlorophyll was extracted from about 0.1 g fresh apical leaves in 25 ml ethanol (95%) in the dark for 48 h at 25 °C. Then, the supernatant was used to measure absorbance on a spectrophotometer at 645 and 663 nm, respectively. The contents of chlorophyll *a* (Chl.a) and chlorophyll *b* (Chl.b) were calculated using the equations of Arnon (1949) and expressed in mg pigments/g fresh weight (Su et al., 2012):

$$\text{Chlorophyll a}\ (\mathrm{mg\ g^{-1}}) = (12.7 \times \mathrm{OD_{663}} - 2.69 \times \mathrm{OD_{645}}) \frac{V}{W \times 1000}$$

$$\text{Chlorophyll b}\ (\mathrm{mg\ g^{-1}}) = (22.9 \times \mathrm{OD_{645}} - 4.68 \times \mathrm{OD_{663}}) \times \frac{V}{W \times 1000}$$

$$\text{Total chlorophyll}\ (\mathrm{mg\ g^{-1}}) = \text{Chlorophyll } a + \text{Chlorophyll } b$$

where V (ml) is the volume of the extracted liquid and W (g) is the fresh weight of the extracted leaves.

The fresh leaf tissue was placed on a glass slide and distilled water was added to make a temporary seal, after which the slide was immediately observed and photographed under a laser scanning confocal microscope (LSCM). The microscope was a Leica SP8, and the confocal system was controlled by Lasersharp software. Then, the blades were placed on an LSCM platform to focus on the most luminous scanning plane of chloroplast spontaneous fluorescence. The excitation wavelength was 488 nm, the receiving range of the emitted light was set to 411–695 nm and the pinhole size was 1 AiryUnit. The scanning resolution (frame size) was 1024 × 1024, the scanning speed 3.15 μs/pixel and the averaging number 2. The results were analysed digitally by Lasersharp software (Paddock, 1999).

2.6. Determination of malondialdehyde (MDA), superoxide radical (O_2^-) and hydrogen peroxide (H_2O_2) in plant leaves

The level of lipid peroxidation in plant leaves was determined by estimation of the MDA content based on the method of Heath and Packer (1968). Briefly, about 0.1 g fresh plant material was ground with 5 ml 1% trichloroacetic acid (TCA). The homogenate was centrifuged at 10,000 rpm for 15 min, after which 0.5 ml of the supernatant was mixed with 2 ml 0.5% thiobarbituric acid in 20% TCA. The mixture was heated at 96 °C for 30 min, stopped at 0 °C and centrifuged at 8000 rpm for 10 min, followed by measurement of absorbance at 450, 532 and 600 nm on a spectrophotometer. The relationship between MDA and OD can be explained using the below equation:

$$\mathrm{MDA}(\mu\mathrm{mol\ g^{-1}}) = [6.45 \times (\mathrm{OD_{532}} - \mathrm{OD_{600}}) - 0.56 \times \mathrm{OD_{450}}] \times \frac{V}{W \times 1000}$$

where V (ml) is the volume of extracted liquid, and W (g) is the fresh weight of the extracted leaves.

The level of O_2^- was determined by measuring the nitrite formed from hydroxylamine in the presence of O_2^- using essentially the method described by Elstner and Heupel (1976), but with some modification. Approx. 0.1 g plant material was homogenised in 10 ml 65 mM potassium phosphate buffer (pH 7.8) and centrifuged at 10,000 rpm for 10 min. Then, 2 ml supernatant was mixed with 1.5 ml 65 mM phosphate buffer (pH7.8) and 0.5 ml 10 mM hydroxylamine hydrochloride and incubated at 25 °C for 20 min. Subsequently, p-aminobenzenesulfonicacid (17 mM final concentration) and naphthylamine (7 mM final concentration) were added to the mixture, which was incubated at 30 °C for 30 min. An equal volume of ethyl ether was added and the mixture was centrifuged at 8000 rpm for 5 min. The absorbance of the aqueous solution at 530 nm was measured. A standard curve with NO_2^- was used to calculate the production rate of O_2^- from the chemical reaction of O_2^- and hydroxylamine.

H_2O_2 was determined as described by Jana and Choudhuri (1982). About 0.1 g plant material was ground in liquid nitrogen and then homogenised in 3 ml 50 mM sodium phosphate buffer (pH 6.5). The homogenate was centrifuged at 8000 rpm for 20 min. For the determination of H_2O_2, 750 μl supernatant was mixed with 2.5 ml 0.1% titanium sulfate in 20% (v/v) H_2SO_4 and centrifuged at 8000 rpm for 10 min. The absorbance of supernatant 415 nm was measured, and the absorbance values were calibrated against a standard curve generated with known concentrations of H_2O_2.

2.7. Determination of catalytic activities of peroxidase enzymes

Peroxidase (POD) activity was determined as oxidation of guaiacol by H_2O_2 (Upadhyaya et al., 1985), but with some modification. About 0.1 g plant material was homogenised in 10 ml distilled water and centrifuged at 8000 rpm for 10 min 1 ml 0.18% H_2O_2, 0.2 ml 0.1% guaiacol, 6.9 ml distilled water and 1 ml enzyme

extract (a blank was made for each set of enzyme extract and 1 ml H_2O_2 was replaced with 1 ml distilled water) were incubated at 25 °C for 10 min, after which 0.2 ml 5% HPO_3 was added to stop the reaction. The increase in absorbance at 470 nm was measured. One unit of POD activity was defined as the amount required to decompose 1 μg $g^{-1}min^{-1}$.

2.8. Determination of dissolved oxygen, the oxidation-reduction potential and SN

Dissolved oxygen (DO) and the oxidation-reduction potential (ORP) of the water were measured with a multi-function water quality determinator (YSI ProPlus, USA). High pressure liquid chromatography (HPLC) (Agielnt 1100 system, USA) was used to analyse the antibiotics in the water samples collected from different treatment groups (Ji et al., 2011), but with some modification. A 1 ml sample of water was filtered through a 0.22 μm membrane filter (Hydrophilic) and used for determination of the residual concentrations of SN in the aqueous medium. A 10 μl sample was injected onto a C18 column (250 × 4.6 mm, 5 μm pore size), while maintaining a column temperature of 40 °C. Acetonitrile and phosphoric acid (60: 40 v/v) were used as the mobile phase at a flow rate of 1 ml min^{-1}. The column effluent was monitored at 259 nm to detect the SN. Calibration curves of six points showed good linearity for the analyte ($R^2 = 0.99$; $P < 0.0001$) in the domain of the expected sample concentration.

The removal rate (RR) of SN by different treatment groups was calculated by the following equation:

$$RR(\%) = \frac{Co - Ct}{Co} \times 100\%$$

where *Co* is the initial concentration of SN at time zero, and *Ct* is the concentration of SN at time t.

2.9. DNA extraction, amplification and MiSeq sequencing

Total bacterial DNA was extracted from samples using the Power Soil DNA Isolation Kit (MO BIO Laboratories) according to the manufacturer's protocol. The quantity and quality of DNA samples were analysed using a Nanodrop spectrophotometer (Nanodrop 2000, Thermo Scientific, USA) (Liu et al., 2017). DNA samples for subsequent tests were stored at −80 °C. The V3–V4 hypervariable regions of 16S rRNA were amplified from microbial genomic DNA and the primer pairs were described as in Zhao et al. (2018). High-throughput sequencing analysis of bacterial rRNA genes was performed on the purified pooled sample using the Illumina Hiseq 2500 platform (2 × 250 paired ends) at Biomarker Technologies Corporation, Beijing, China.

2.10. Statistical analysis

Growth indicators (RGR, leaf length, root length), physiological indicators (chlorophyll, autofluorescence of chloroplast, MDA, O_2^-, H_2O_2 and POD), DO, ORP, removal rate of SN and SN concentration were analysed with one-way analysis of variance (ANOVA). Fisher's Least Significant Difference (LSD) test was applied to test for the difference in the environmental data and the homogeneity of variances (Levene's test). Otherwise, significance was tested using Dunnett's in post hoc multiple comparisons. Each result shown in the figures is the mean of at least three replicated treatments. Standard deviation and Student's t-test were used to examine the differences between treatments and the level of statistical significance was set to $p^*0.05$. One-way ANOVA was completed by IBM SPSS Statistics for Windows (version 18, Chicago, IL, USA). Graphical work was carried out using Origin 9.0 (OriginLab Corporation, Northampton, MA, USA).

The overlapping regions between the paired-end reads were merged using FLASH v1.2.7 and primer sequences were trimmed after the raw sequences were denoised, sorted and separated using Trimmomatic (version 0.33). Sequences that were less than 200 bp in length or contained homopolymers longer than 8 bp were removed. The chimera sequences were detected by comparing tags with the reference database (RDP Gold database) using the UCHIME algorithm and then removed. The effective sequences were then used in the final analysis.

Sequences were grouped into operational taxonomic units (OTUs) using the clustering program UCLUST (version 1.2.22) (Edgar, 2010) against the SILVA bacterial database (Quast et al., 2012) pre-clustered at 97% sequence identity. Shannon-Wiener indices were calculated by Mothur (version v.1.30) from rarefied samples using richness and diversity indices of the bacterial community. Beta diversity was calculated applying unweighted UniFrac and principal coordinate analysis (PCoA), after which Intra-group and Inter-group beta distance boxplot diagrams were generated. A one-way analysis of similarity (ANOSIM) was performed to determine the differences in bacterial communities among groups (Clarke and Gorley, 2006). Linear discriminant analysis (LDA) effect size (LefSe) analysis was performed to reveal the significant ranking of abundant modules. A size-effect threshold of 4.0 on the logarithmic LDA score was used for discriminative functional biomarkers. LefSe was performed online in the Galaxy workflow framework 2.0.

Alpha diversity indexes are presented as the mean ± SD. The differences in Alpha diversity indexes and top 10 phyla and genera relative abundances between groups were calculated by use of the Independent-sample *t*-test (for the normally distributed data) or Mann-Whitney *U* test (for the non-normally distributed data). A P-value < 0.05 was considered statistically significant.

3. Results

3.1. Effects of SN on the growth of V. natans

The mean leaf length of *V. natans* in all treatments on day 10 and day 20 was significantly higher than on day 0 ($p < 0.05$). On day 20, the treatment with 50 mg L^{-1} SN had led to a significant decrease in mean leaf length compared with 0 and 10 mg L^{-1} SN ($p < 0.05$), while no significant alteration in mean leaf length was observed in the 30 and 50 mg L^{-1} SN treatments ($p > 0.05$). (Fig. 1a).

On day 10, the mean root length of the control was significantly higher than that of *V. natans* treated with 30 and 50 mg L^{-1} SN ($p < 0.05$), while no significant alteration in mean root length was observed in *V. natans* treated with 10, 30 and 50 mg L^{-1} SN ($p > 0.05$). On day 20, the mean root length of the control was significantly higher than that of *V. natans* treated with 10, 30 and 50 mg L^{-1} SN ($p < 0.05$), while there was no significant difference in mean root length among the 10, 30 and 50 mg L^{-1} SN treatments ($p > 0.05$) (Fig. 1b).

RGR decreased with the increase of SN concentrations; the highest concentration of SN resulting in the lowest RGR (Fig. 1c). SN had significant effects on RGR. Compared with the control, RGR was significantly reduced at 30 and 50 mg L^{-1} ($p < 0.05$). No significant difference was observed between the control and the 10 mg L^{-1} SN groups ($p > 0.05$).

3.2. Effects of SN on the photosynthetic system

SN concentrations greater than 10 mg L^{-1} disrupted the normal chlorophyll content of *V. natans* ($p < 0.05$), while there was no

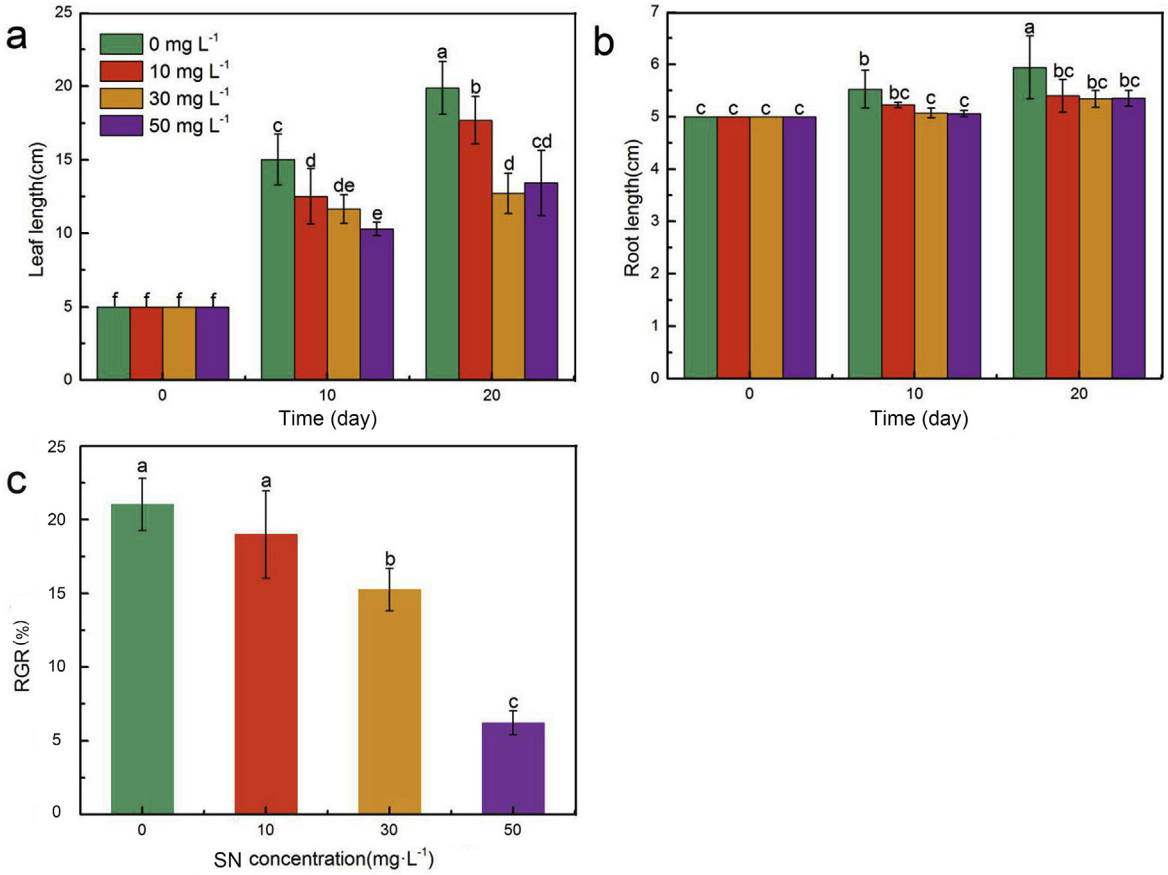

Fig. 1. Differences in (a) leaf length and (b) root length in the four SN treatments on day 0, 10 and 20, respectively. Average relative growth rate (RGR) (%) on day 20 of the experiment (c). Data are shown as mean ± SD (n = 4); different letters represent significant differences at the $p < 0.05$ level.

significant alteration when SN ranged between 0 and 10 mg L^{-1} ($p > 0.05$) (Table 1). Compared with the control, autofluorescence of chloroplast decreased significantly in *V. natans* exposed to 10, 30 and 50 mg L^{-1} SN on day 10 and 20 of the experiment ($p < 0.05$). On both day 10 and day 20, the autofluorescence of chloroplast was lowest at 50 mg L^{-1} SN (Fig. 2). The number of the chloroplasts and the degree of damage of the chloroplasts were represented by the number and brightness of red highlights, respectively. The highest concentration of SN resulted in the most severely damaged chloroplast (Fig. 3).

3.3. Effects of SN on MDA, POD, H_2O_2 and O_2^- in leaves of V. natans

The MDA content exhibited a significant increase on day 20 compared with day 0 ($p < 0.05$). There was no significant difference on day 0 and 10 of the experiment ($p > 0.05$). The MDA content with 50 mg L^{-1} SN was significantly higher than that with 0, 10 and 30 mg L^{-1} ($p < 0.05$) on day 20 (Fig. 4a).

The H_2O_2 concentration had increased significantly in the *V. natans* leaves in all treatments on day 10 and day 20 compared with day 0 ($p < 0.05$). No significant alteration in H_2O_2 concentrations was observed in *V. natans* leaves treated with 10, 30 and 50 mg L^{-1} SN after 20 days ($p > 0.05$), while there was a significant ($p < 0.05$) difference between the control and the treatments (Fig. 4b).

A significant increase of O_2^- concentrations was observed in *V. natans* leaves treated with 10, 30 and 50 mg L^{-1} SN for 10 and 20 days compared with the control ($p < 0.05$) (Fig. 4c). After 20 days' exposure, the O_2^- concentration in *V. natans* leaves with 50 mg L^{-1} SN was significantly ($p < 0.05$) higher than that with 0, 10 and 30 mg L^{-1} SN, while no significant alteration was observed in *V. natans* leaves treated with 10 and 30 mg L^{-1} SN ($p > 0.05$).

Compared with the control, the POD activity of *V. natans* had increased significantly in the treatments with 30 and 50 mg L^{-1} ($p < 0.05$) on day 10 and day 20. The change in the POD enzymatic activity with different SN concentrations showed a similar trend as MDA (Fig. 4d).

Table 1
Contents of chl.a, chl.b and total chlorophyll in *V. natans* (men ± SD, n = 4) grown at different SN concentrations and ANOVA (*F*-ratios) results on day 20. Different letter superscripts between columns indicate significant differences between treatments ($p < 0.05$).

SN concentration	Chl.a (mg g^{-1} FW)	Chl.b (mg g^{-1} FW)	Total chlorophyll (mg g^{-1} FW)
0 mg L^{-1}	0.95 ± 0.08^{a}	0.38 ± 0.04^{a}	1.32 ± 0.12^{a}
10 mg L^{-1}	0.93 ± 0.21^{a}	0.37 ± 0.07^{a}	1.29 ± 0.27^{a}
30 mg L^{-1}	0.67 ± 0.21^{ab}	0.28 ± 0.11^{ab}	0.95 ± 0.32^{ab}
50 mg L^{-1}	0.52 ± 0.21^{b}	0.17 ± 0.10^{b}	0.69 ± 0.27^{b}
F-ratio	5.1*	5.76*	5.82*

*$P < 0.05$.

3.4. Dynamics of DO and ORP in the water column

DO levels of the three different treatments were similar at the beginning of the experiment (6.61 ± 0.39 mg L^{-1}). During the first 8 days of the experiment, the DO of all treatments showed a rapid decline. Among the treatments, on days 8–13, the highest DO was

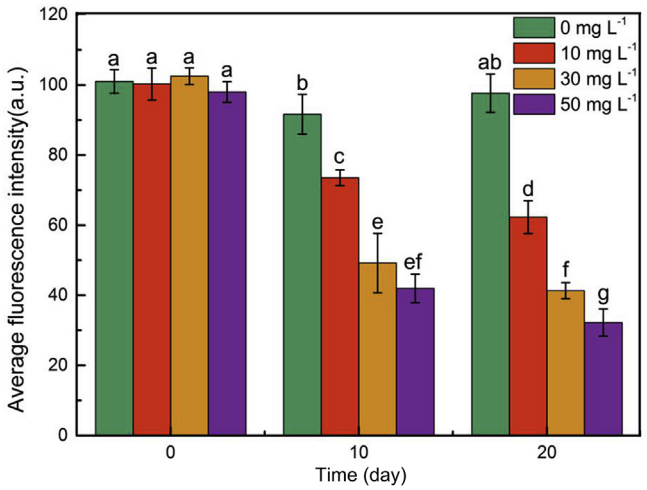

Fig. 2. Average autofluorescence intensity on day 0, 10 and 20 of the experiment. Data are shown as the mean ± SD (n = 4); different letters represent significant differences between treatments at $p < 0.05$.

observed in treatment V + S-. A relatively lower DO was found in treatment V + S+. The lowest DO was recorded in treatment V−S+. There was a significant difference ($p < 0.05$) in DO among all treatments on days 8−11 (Fig. 5a). The changes in ORP were similar to those in DO. Also during the period days 8−13, the trend of treatment V + S- > treatment V + S+> treatment V−S+ appeared, and there was a significant difference between the treatments ($p < 0.05$) (Fig. 5b).

3.5. Dynamics of SN in the water column

The SN concentration remained essentially unchanged until day 3. Thereafter, the concentration decreased rapidly. On day 11, the SN concentration in the V+S+ treatment was about 0.16 ± 0.01 mg L^{-1}, which was significantly lower than in the V−S+ treatment ($p < 0.05$). After day 13, the detected concentrations of SN were below 0.10 mg L^{-1} in all treatments (Fig. 6a). Removal of SN from the water in the different treatments over time is presented in Fig. 6b. On day 9 and day 11, the removal rate in the V+S+ treatment was significantly higher than in the V−S+ treatment ($p < 0.05$).

3.6. Microbial community

A total of 1,169,143 high-quality microbial sequences were identified from all the samples. The rarefaction curves for the OTUs detected and post-filtering sequencing data in this study are displayed in Supplementary Table S3 and Fig. S2. The numbers of OTUs, Shannon-Wiener indices and PCoA showed extremely significant differences in bacterial communities between the treatments (Fig. 7 and Fig. S3).

The identified bacterial structures and relative abundances are shown in Fig. 8a and b at phylum and order level, respectively. The dominant phyla were *Proteobacteria*, *Bacteroidetes* and *Actinobactcria*, followed by *Patescibacteria* and *Verrucomicrobia* (Fig. 8a). SN increased the relative abundance of *Patescibacteria,*

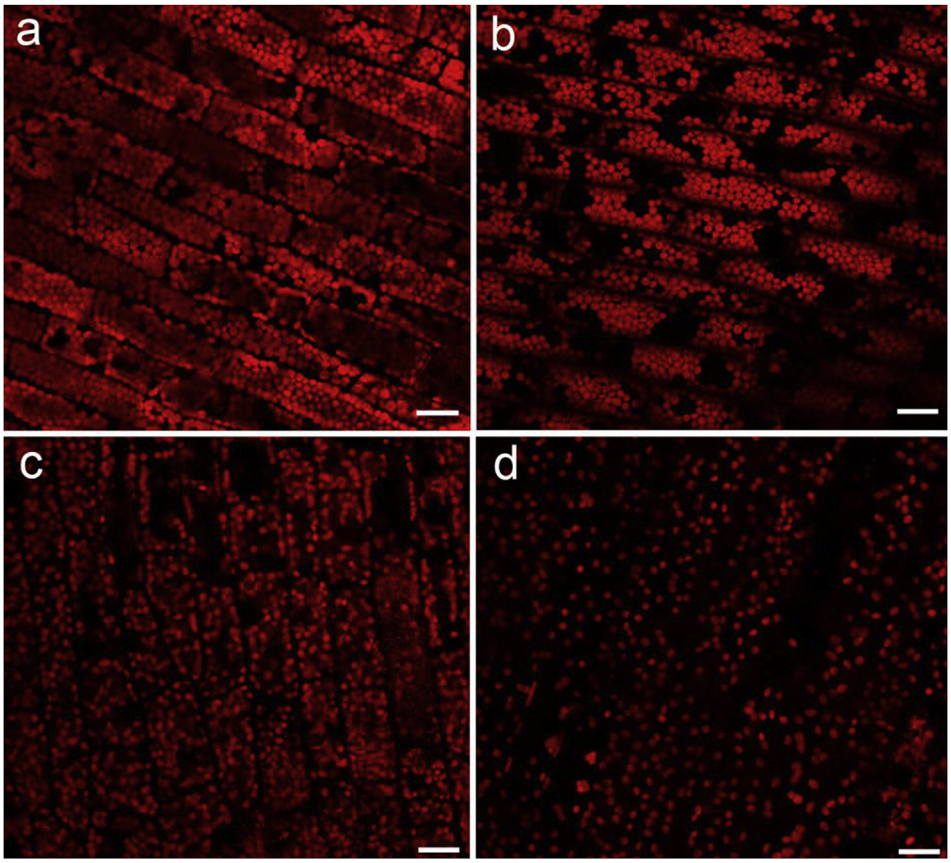

Fig. 3. Chloroplast fluorescence photos of *V. natans* at different levels of the SN treatment by the end of the experiment (20 day). SN concentrations are 0 mg L^{-1} (a), 10 mg L^{-1} (b), 30 mg L^{-1} (c) and 5 0 mg L^{-1} (d). Scale bar = 25 μm.

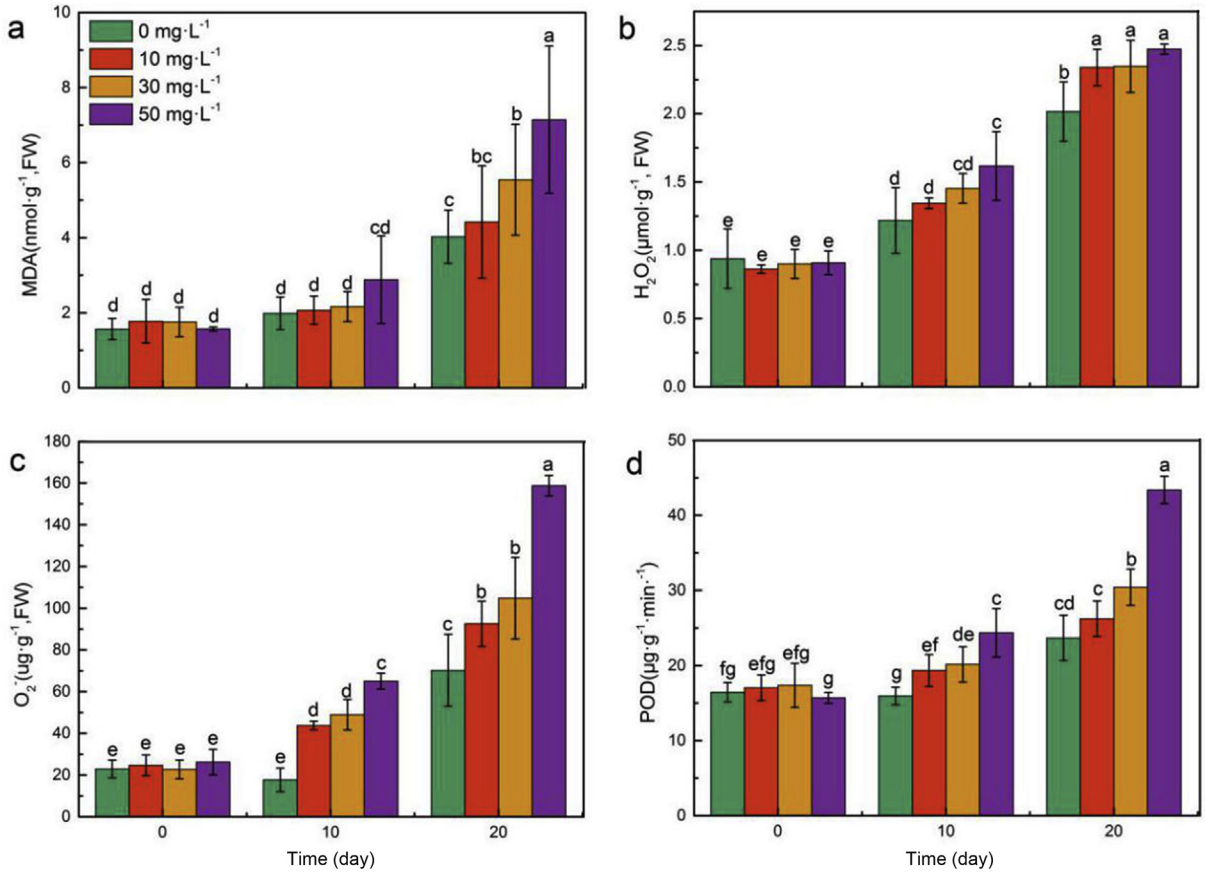

Fig. 4. Effects of SN on MDA (a), H_2O_2 (b), O_2^- (c) and POD (d) in leaves of *V. natans*. Data are shown as mean ± SD (n = 4); different letters represent significant differences at $p < 0.05$.

Actinobactcria and *Cyanobacteria* in the periphyton samples and the abundance of *Patescibacteria* in the water samples. The presence of *V. natans* increased the relative abundance of *Patescibacteria* in the water samples, while SN decreased the relative abundance of *Verrucomicrobia*, *Proteobacteria* and *Bacteroidetes* (Fig. 8a).

The dominant orders were *Betaproteobacteriales*, *Micrococcales* and *Saccharimonadales*. SN increased the relative abundance of *Saccharimonadales, Sphingobacteriales* and *Micrococcales* in the periphyton samples and *Saccharimonadales* and *Rhizoniales* in the water samples. The presence of *V. natans* increased the relative

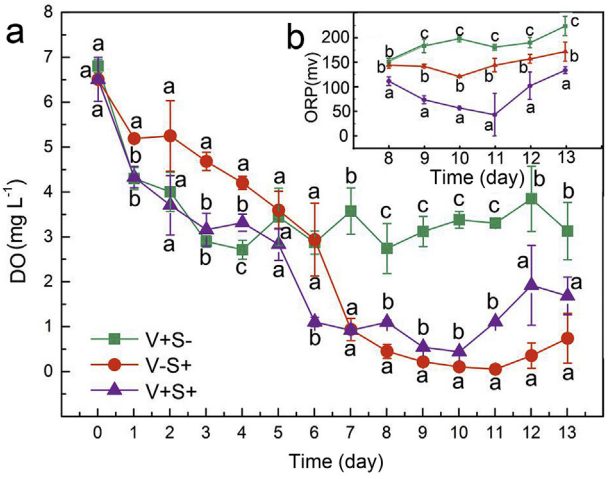

Fig. 5. The variation of DO (dissolved oxygen) (a) and the oxidation-reduction potential (ORP) (b) in different treatments with time. Data are shown as mean ± SD (n = 4); different letters represent significant differences between treatments at $p < 0.05$. (V + S-: *V. natans* and no SN; V−S+: no *V. natans* and SN; V + S+: *V. natans* and SN).

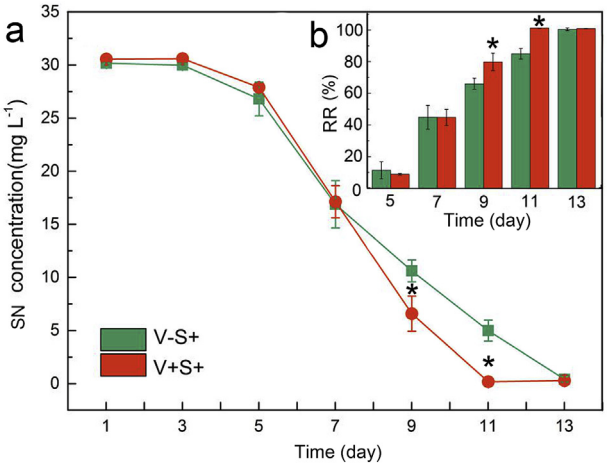

Fig. 6. The concentration of SN with time (a). RR of SN in the different treatments (b). Data are shown as mean ± SD (n = 4). Values are significantly different (ANOVA/Paired-Samples T Test) from the blank controls at the same time as indicated by asterisk (*$p < 0.05$). (V−S+: no *V. natans* and SN; V + S+: *V. natans* and SN).

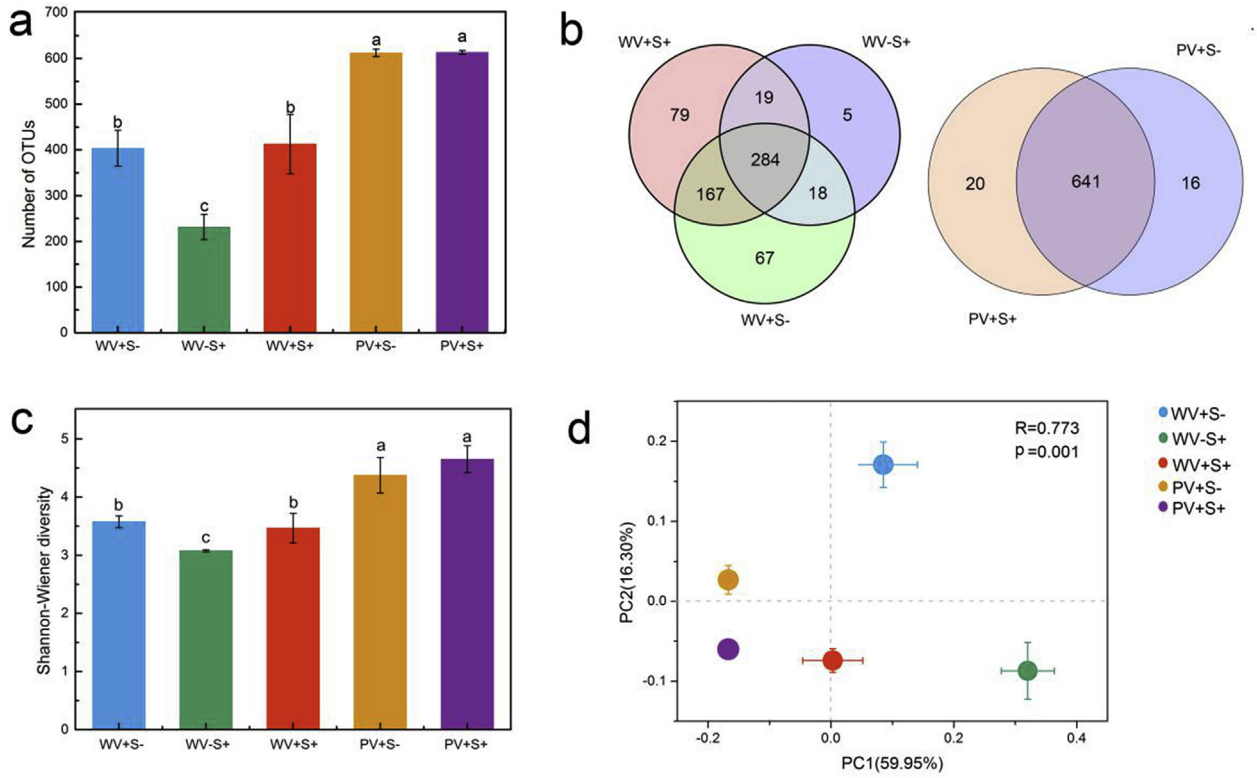

Fig. 7. (a) Number of OTUs in different treatments; (b) Venn diagrams. The Venn diagrams show the numbers of OTUs (97% sequence identity) that were shared or not shared; (c) Shannon-Wiener diversity in different treatments; (d) PCoA of unweighted UniFrac distances as a measure of beta diversity across samples. Data are shown as mean ± SD ($n \geq 3$). Different letters represent significant differences at $p < 0.05$ between treatments. (WV + S-: Water sample, *V. natans* and no SN; WV-S+: Water sample, no *V. natans* and SN; WV + S+: Water sample, *V. natans* and SN; PV + S-: Periphyton sample, *V. natans* and no SN; PV + S+: Periphyton sample, *V. natans* and SN).

abundance of *Saccharimonadales* and *Rhizoniales* in the water samples, while SN led to a reduction of the relative abundance of *Chitinophagales*, *Betaproteobacteriales* and *Flavobacteriales* (Fig. 8b).

LefSe analysis was performed to reveal the significant ranking of abundant modules. The cladogram showed differences in WV-S+ and WV + S+ (Fig. 8c), PV + S- and PV + S+ (Fig. 8d), respectively. The plot from LefSe analysis displays LDA scores of microbial taxa with significant differences in WV-S+ and WV + S+ (Fig. S4a), PV + S- and PV + S+ (Fig. S4b), respectively. At order level, the biomarkers demonstrating significant differences between the WV-S+ and WV+S+ were *Saccharimonadales*, *Flavobacteriales* and *Pseudomonadaceae*, and between the PV + S- and PV+S+ the biomarkers displaying differences were *Saccharimonadales*, *Micrococcales*, *Sphingobacteriales*, *Bacteroidales*, *Obscuribacterales* and *Myxococcales*.

4. Discussion

4.1. Ecotoxicological effects of SN

Our results indicated that high SN had toxic effects on the growth and physiological metabolism of *V. natans*. Leaves are organs for photosynthesis and under the condition of stress, the photosynthesis efficiency will decrease, inhibiting the growth and development of plants and the synthesis of Chl.a and Chl.b (Wang et al., 2011). Previous research has indicated that autofluorescence intensity was closely related to the chlorophyll content (Paddock, 1999), and the chlorophyll variation trend of *V. natans* and *Phragmites communis* observed under the stress of oxytetracycline, tetracycline and sulfamethazine was similar to that of our study (Table 1) (Jiao et al., 2008; Lin et al., 2013). In addition, ROS (O_2^-, OH and H_2O_2) are toxic to plant cells because they can rapidly attack chloroplasts, nucleic acid, proteins and membrane lipids (Apel and Hirt, 2004). Moreover, being a lipid peroxide, MDA levels can indirectly reflect the severity of free radical attacks, and MDA can thus reflect the degree of stress injury to plants (Nimptsch and Pflugmacher, 2007). Our results indicated that high SN had toxic effects on the physiological metabolism and caused structural and functional damage in *V. natans* (Fig. 1a-b, Figs. 3 and Fig. 4a–c).

Despite the toxic effects, *V. natans* was overall rather resistant to SN as the plant biomass still increased significantly compared with the initial period with high SN (Fig. 1c). POD can decompose H_2O_2 to water and oxygen and is found in the cytosol, the cell wall and in vacuolar and extracellular spaces (Mishra et al., 2006). The stimulated activity of POD in the SN-treated leaves reflected an enhanced degree of antioxidative response in *V. natans* to resist the oxidative stress (Fig. 4d). Several cellular processes such as aerobic respiration and photosynthesis can produce reactive oxygen species (ROS: superoxide (O_2^-), hydrogen peroxide (H_2O_2), hydroxyl radical ($\cdot OH$), singlet oxygen ($^1O_2$)) (Baxter et al., 2014) that play important physiological roles in plant development and defence (Cona et al., 2006). Previous research has indicated that an increased chlorophyll content in microalgal cells reflects that chlorophyll acts as a protective agent to neutralise the accumulated ROS in chloroplast (Xiong et al., 2016). Therefore, we speculate that the chlorophyll content in *V. natans* cells has a similar function. In addition, MDA can also serve as an indicator of several different enzymes (NADPH-dependent oxidase, peroxidases) (Apel and Hirt, 2004). These enzymes can effectively transform the accumulated contaminants intracellularly through various enzymatic systems (Tang et al.,

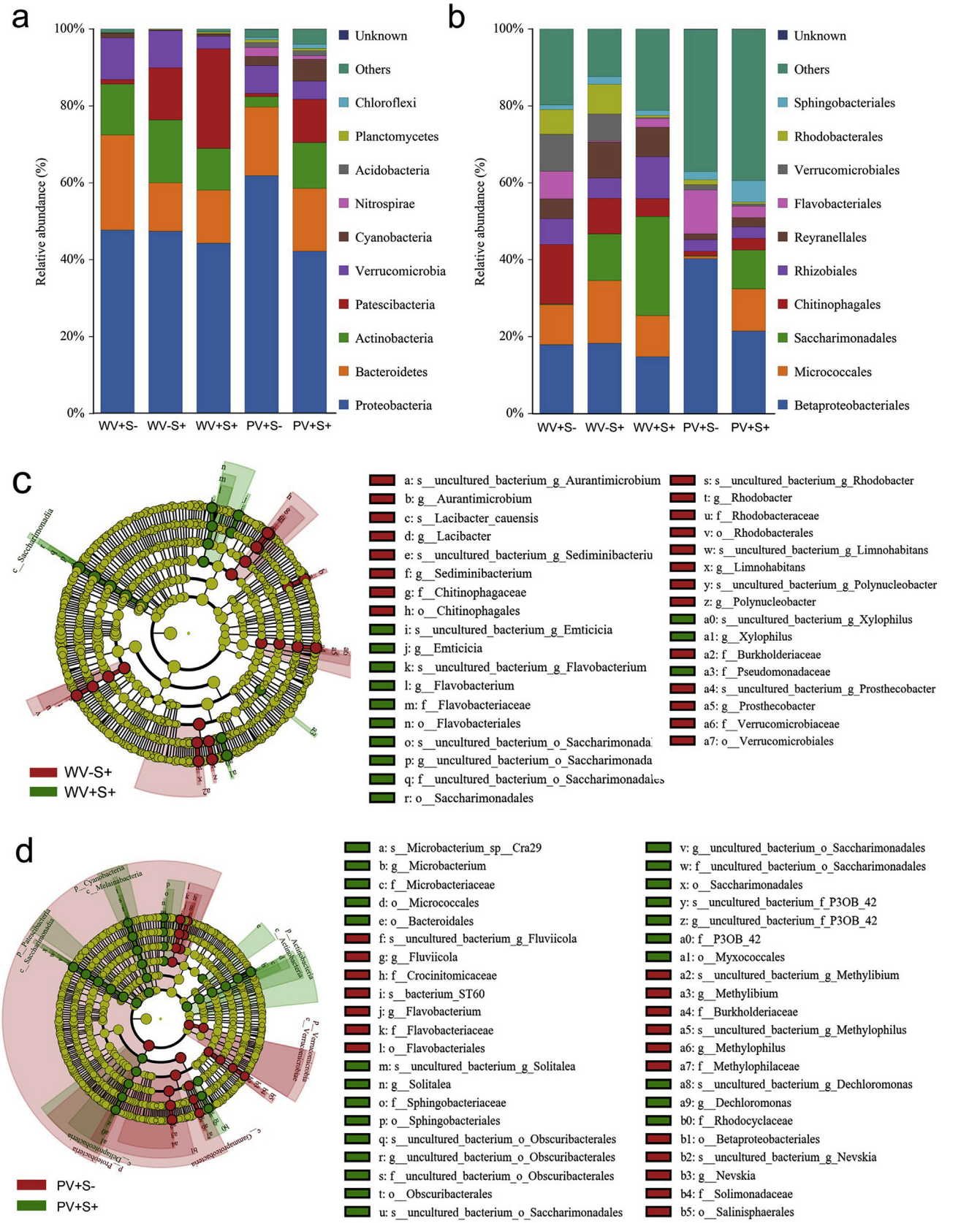

Fig. 8. Microbial population dynamics at different levels. (a) Relative abundance of the top 10 phyla. (b) Relative abundance of the top 10 order. Data are shown as means ($n \geq 3$). Only the abundances of the top 10 species are shown in the figure, other species were combined as "Others." LefSe analysis. (c): WV-S+ and WV + S+, (d): PV + S- and PV + S+. The cladogram diagram shows the microbial species displaying significant differences in the two groups. Red and green indicate different groups, species classification being shown At the level of phylum, class, order, family and genus from the inside to the outside. (WV + S-: Water sample, *V. natans* and no SN; WV-S+: Water sample, no *V. natans* and SN; WV + S+: Water sample, *V. natans* and SN; PV + S-: Periphyton sample, *V. natans* and no SN; PV + S+: Periphyton sample, *V. natans* and SN). (For interpretation of the references to colour in this figure legend, the reader is referred to the Web version of this article.)

2016). Our experiment was run at high SN concentrations compared with typical concentrations in the field. The toxicological effects on the plants, though modest in our study, are, therefore, expected to be markedly lower under field conditions.

4.2. Removal of SN by *V. natans*

Our results indicate that the presence of *V. natans* changed the redox environment of the water body by increasing DO and ORP, which likely favouring the removal of SN (Figs. 5 and 6). Several studies have shown that the plant community via photosynthesis can enhance DO to saturation levels of 150–200% in highly productive streams (Thomann and Mueller, 1987) with implications also for the redox status (Li and Bishop, 2002) and decomposition of organic matter (Yadav et al., 2014). Moreover, some macrophytes (e.g. *Pistia stratiotes*, *Myriophyllum aquaticum)* have been shown to release reactive oxygen species in root exudates that may inactivate tetracycline (TC) and oxytetracycline (OTC) (Gujarathi et al., 2005). Previous research has shown that pollutants (TN, TP, BOD_5 and COD) can be removed by hydroxyl radicals (Zhuang et al., 2014). Some studies of the photocatalytic decomposition of SAs have reported that the degradation reaction was mainly initiated via hydroxylation by hydroxyl radicals (Yan et al., 2011). In an investigation, degradation of sulfamonomethoxine (SMM) was found to be initiated by hydroxylation of the phenyl and pyrimidinyl portions, transformation of a NH_2 group into a NO group and substitution of the OCH_3 group with an OH group (Nomura et al., 2017). Moreover, Zhang et al. (2018) found that *V. natans* can repair polycyclic aromatic hydrocarbons (PAHs) by increasing ORP in sediments. In our study, although the content of ROS (H_2O_2 and O_2^-) in the water column was not determined, we measured the changes of ROS content in the body of *V. natans* in the first toxicological experiment (Fig. 4b and c) and those of ORP in the SN removal experiment (Fig. 5b). The corresponding increase of these parameters may also be the reasons for the decrease of SN.

Biodegradation (microbial transformation) has been proposed to play the major role in SAs removal (Müller et al., 2013; Yang et al., 2012). In the present study, SN and the presence of *V. natans* increased the relative abundance of *Saccharimonadales*, *Flavobacteriales*, *Rhizoniales*, *Micrococcales*, *Sphingobacteriales*, *Bacteroidales*, *Obscuribacterales*, *Myxococcales* and *Pseudomonadaceae* (Fig. 8). A previous study has shown that *Pseudomonadaceae*, *Flavobacteriales*, and *Sphingobacteriales* are aerobic bacteria (Yan et al., 2015). In our study, the presence of *V. natans* may favoured these by the higher DO level, supporting the dominance of these microbes. So far, a few SAs-degrading microorganisms have been isolated and characterised, including *Pseudomonas* (Jiang et al., 2014) and *Myxococcales* (Birkigt et al., 2015; Müller et al., 2013). Moreover, *Acinetobacter* (*Myxococcales* and *Bacteroidales*) isolated from marine environments have been reported to be involved in sulfapyridine and sulfathiazole degradation (Zhang et al., 2012). Three orders (i.e., *Myxococcales*, *Sphingobacteriales* and *Flavobacteriales*) have been reported to be associated with the degradation of organic pollutants such as aromatic hydrocarbons (Alonso-Gutiérrez et al., 2009; Yang et al., 2016; Zhang et al., 2010). We found the diversity of bacteria to be higher in the treatment with than without *V. natans* (Fig. 7c) and the higher bacterial diversity may have favoured SN removal. Studies of the removal of pharmaceuticals and personal care products (PPCPs) have revealed similar results (Kang et al., 2018).

Our study used aquatic macrophytes and microorganisms as the main research objects to provide new insight into the degradation of SAs in natural waters. Some studies have shown that photolysis appears to be the main degradation process of SAs in natural waters (Andreozzi et al., 2003). Others have found that also plant enrichment and adsorption are pathways for SAs degradation, but adsorption and accumulation levels are relatively low ($\mu g\ Kg^{-1}$) and not considered to be their main removal route (Choi et al., 2008; Senta et al., 2013; Bao et al., 2010; Xian et al., 2010). Moreover, enzymes (cytochrome P450 enzyme families, glutathione-S-transferases and laccase) of microalgae are actively involved in the degradation of xenobiotic organic pollutants (Kurade et al., 2016; Mellor et al., 2016; Xiong et al., 2016). *V. natans* may use a similar route to degrade SN, which needs further investigation.

5. Conclusion

Our study showed that SN had toxic effects on the growth of *V. natans*, but that *V. natans* was relatively resistant to SN, showing net growth at all doses of SN. *V. natans* significantly improved the removal efficiency of SN in the water column. SN removal was related to the ORP conditions and diversity of the bacterial community triggered by *V. natans*. SN and the presence of *V. natans* increased the relative abundances of *Saccharimonadales*, *Flavobacteriales*, *Rhizoniales*, *Micrococcales*, *Sphingobacteriales*, *Bacteroidales*, *Obscuribacterales*, *Myxococcales* and *Pseudomonadaceae*, which are all considered to be SN-resistant bacteria.

Our results add to the understanding of the antibiotic removal mechanism of macrophytes in freshwater systems, but further experimental studies are needed to clarify the exact mechanisms behind the interaction between antibiotics and the macrophyte-microorganism systems, for example by studying the variation of specific epiphytic and pelagic eukaryotic microorganisms and bacterial species under laboratory culture conditions.

Declaration of competing interest

The authors declare that they have no known competing financial interests or personal relationships that could have appeared to influence the work reported in this paper.

Acknowledgements

This research was supported by projects of the National Water Pollution Control and Treatment Science and Technology Major Project (2017ZX07207002), the National Key R&D Program of China (2017YFD0701700), Science and Technology Commission of Shanghai Municipality (19050501900 and 19DZ1204504) and the 63rd China Postdoctoral Science Foundation (2018M632099). We thank all the students at the laboratory of aquatic ecology and environmental restoration from Shanghai Ocean University for laboratory assistance. We also would like to express our deep thanks to Anne Mette Poulsen from Aarhus University for her English assistance.

Appendix A. Supplementary data

Supplementary data to this article can be found online at https://doi.org/10.1016/j.watres.2019.115354.

References

Alonso-Gutiérrez, J., Figueras, A., Albaigés, J., Jiménez, N., M, Vinas, A., Solanas, M., Novoa, B., 2009. Bacterial communities from shoreline environments (Costa da Morte, Northwestern Spain) affected by the Prestige oil spill. Appl. Environ. Microbiol. 75 (11), 3407–3418.

Arnon, D.I., 1949. Copper enzymes in isolated chloroplasts: polyphenoloxidase in Beta vulgaris. Plant Physiol. 24 (1), 1–15.

Andreozzi, R., Raffaele, M., Nicklas, P., 2003. Pharmaceuticals in STP effluents and their solar photodegradation in aquatic environment. Chemosphere 50 (10), 1319–1330.

Apel, K., Hirt, H., 2004. Reactive oxygen species: metabolism, oxidative stress, and

signal transduction. Annu. Rev. Plant Biol. 55 (1), 373–399.
Bao, X.B., Qiang, Z.M., Ben, W.W., 2013. Adsorptive removal of sulfonamides from water by magnetic nanocomposite CoFeM48. Acta Sci. Circumstantiae 33 (2), 401–407.
Bao, Y.P., Li, Y.W., Mo, C.H., Yao, Y., Tai, Y.P., Wu, X.L., Zhang, Y., 2010. Determination of six sulfonamide antibiotics in vegetables by solid phase extraction and high performance liquid chromatography. Environ. Chem. 29 (3), 513–518.
Baxter, A., Mittler, R., Suzuki, N., 2014. ROS as key players in plant stress signalling. J. Exp. Bot. 65 (5), 1229–1240.
Białk-Bielińska, A., Stolte, S., Arning, J., Uebers, U., Böschen, A., Stepnowski, P., Matzke, M., 2011. Ecotoxicity evaluation of selected sulfonamides. Chemosphere 85 (6), 928–933.
Birkigt, J., Gilevska, T., Ricken, B., Richnow, H., Vione, D., Corvini, P.F., Nijenhuis, I., Cichocka, D., 2015. Carbon stable isotope fractionation of sulfamethoxazole during biodegradation by *Microbacterium* sp. strain BR1 and upon direct photolysis. Environ. Sci. Technol. 49 (10), 6029–6036.
Chen, G.L., Liu, X.M., Xu, J.M., Brookes, P.C., Wu, J.J., 2014. Arsenic species uptake and subcellular distribution in *Vallisneria natans* (Lour.) Hara as influenced by aquatic pH. Bull. Environ. Contam. Toxicol. 92 (4), 478–482.
Choi, K., Kim, Y., Park, J., Park, P.C., Kim, M.Y., Kim, S.O., Kim, P., 2008. Seasonal variations of several pharmaceutical residues in surface water and sewage treatment plants of Han River, Korea. Sci. Total Environ. 405 (1–3), 120–128.
Clarke, K.R., Gorley, R.N. (Eds.), 2006. PRIMER V6: User Manual/tutorial (Plymouth).
Cona, A., Rea, G., Angelini, R., Federico, R., Tavladoraki, P., 2006. Functions of amine oxidases in plant development and defense. Trends Plant Sci. 11 (2), 80–88.
Edgar, R.C., 2010. Search and clustering orders of magnitude faster than BLAST. Bioinformatics 26 (19), 2460–2461.
Eggen, T., Asp, T.N., Grave, K., Hormazabal, K., 2011. Uptake and translocation of metformin, ciprofloxacin and narasin in forage-and crop plants. Chemosphere 85 (1), 26–33.
Elstner, E.F., Heupel, A., 1976. Inhibition of nitrite formation from hydroxylammoniumchloride: a simple assay for superoxide dismutase. Anal. Biochem. 70 (2), 616–620.
Gao, J.P., Garrison, A.W., Hoehamer, C., Mazur, C.S., Wolfe, N.L., 2000. Uptake and phytotransformation of organophosphorus pesticides by axenically cultivated aquatic plants. J. Agric. Food Chem. 48 (12), 6114–6120.
García-Galán, M.J., Díaz-Cruz, M.S., Barceló, D., 2008. Identification and determination of metabolites and degradation products of sulfonamide antibiotics. Trac. Trends Anal. Chem. 27 (11), 1008–1022.
García-Galán, M.J., Díaz-Cruz, M.S., Barceló, D., 2009. Combining chemical analysis and ecotoxicity to determine environmental exposure and to assess risk from sulfonamides. Trac. Trends Anal. Chem. 28 (6), 804–819.
García-Galán, M.J., Blanco, S.G., Roldán, R.L., Díaz-Cruz, S., Barceló, D., 2012. Ecotoxicity evaluation and removal of sulfonamides and their acetylated metabolites during conventional wastewater treatment. Sci. Total Environ. 437, 403–412.
Gujarathi, N.P., Haney, B.J., Linden, J.C., 2005. Phytoremediation potential of *Myriophyllum aquaticum* and *Pistia stratiotes* to modify antibiotic growth promoters, tetracycline, and oxytetracycline, in aqueous wastewater systems. Int. J. Phytoremediation 7 (2), 99–112.
Heath, R.L., Packer, L., 1968. Photoperoxidation in isolated chloroplasts: I. Kinetics and stoichiometry of fatty acid peroxidation. Arch. Biochem. Biophys. 125 (1), 189–198.
Jana, S., Choudhuri, M.A., 1982. Glycolate metabolism of three submersed aquatic angiosperms during ageing. Aquat. Bot. 12, 345–354.
Ji, X.L., Liu, F., Shen, Q.H., Liu, Y., 2011. Quantitative detection of sulfonamides and tetracycline antibiotics and resistance genes in sewage farms. Ecol. Environ. Sci. 20 (5), 927–933.
Jiang, B.C., Li, A., Cui, D., Cai, R., Ma, F., Wang, Y.N., 2014. Biodegradation and metabolic pathway of sulfamethoxazole by *Pseudomonas psychrophila* HA-4, a newly isolated cold-adapted sulfamethoxazole-degrading bacterium. Appl. Microbiol. Biotechnol. 98 (10), 4671–4681.
Jiao, S.J., Dou, Y.Y., Chen, L.Y., Pu, H.Q., Zheng, S.R., Yin, D.Q., 2008. Effect of aqueous tetracycline on *Vallisneria natans* in growth and ultrastructure. Environ. Chem. 27 (3), 335–338.
Kamal, M., Ghaly, A.E., Mahmoud, N., CoTé, R., 2004. Phytoaccumulation of heavy metals by aquatic plants. Environ. Int. 29 (9), 1029–1039.
Kang, D., Zhao, Q.C., Wu, Y.H., Wu, C.X., Wu, X., 2018. Removal of nutrients and pharmaceuticals and personal care products from wastewater using periphyton photobioreactors. Bioresour. Technol. 248, 113–119.
Kümmerer, K., 2009. Antibiotics in the aquatic environment-a review-part II. Chemosphere 75 (4), 435–441.
Kurade, M.B., Kim, J.R., Govindwar, S.P., Jeon, B.H., 2016. Insights into microalgae mediated biodegradation of diazinon by *Chlorella vulgaris*: microalgal tolerance to xenobiotic pollutants and metabolism. Algal Res. 20, 126–134.
Li, B., Bishop, P., 2002. Oxidation-reduction potential (ORP) regulation of nutrient removal in activated sludge wastewater treatment plants. Water Sci. Technol. 46 (1–2), 35–38.
Li, H.T., Pan, Y., Wang, Z.Z., Chen, S., Guo, R.X., Chen, J.Q., 2015. An algal process treatment combined with the fenton reaction for high concentrations of amoxicillin and cefradine. RSC Adv. 5 (122), 100775–100782.
Li, S., Shi, W.Z., Liu, W., Li, H.M., Zhang, W., Hu, J.R., Ke, Y.C., Sun, W.L., Ni, J.R., 2018. A duodecennial national synthesis of antibiotics in China's major rivers and seas (2005 - 2016). Sci. Total Environ. 615, 906–917.
Lin, L., Liu, Y.H., Liu, C.X., Wang, Z., Dong, J., Zhu, G.F., Huang, X., 2013. Potential effect and accumulation of veterinary antibiotics in *Phragmites australis* under hydroponic conditions. Ecol. Eng. 53, 138–143.
Liu, C.J., Xie, J.Z., Song, M.L., Gao, Z.L., Zheng, D.X., Liu, X., Ning, G.H., Cheng, X., Bruning, H., 2017. Nitrogen removal performance and microbial community changes in subsurface wastewater infiltration systems (SWISs) at low temperature with different bioaugmentation strategies. Bioresour. Technol. 250, 603–610.
Mellor, S.B., Nielsen, A.Z., Burow, M., Motawia, M.S., Jakubauskas, D., Møller, B.L., Jensen, P.E., 2016. Fusion of ferredoxin and cytochrome P450 enables direct light-driven biosynthesis. ACS Chem. Biol. 11 (7), 1862–1869.
Migliore, L., Cozzolino, S., Fiori, M., 2003. Phytotoxicity to and uptake of enrofloxacin in crop plants. Chemosphere 52 (7), 1233–1244.
Mishra, S., Srivastava, S., Tripathi, R.D., Kumar, R., Seth, C.S., Gupta, D.K., 2006. Lead detoxification by coontail (*Ceratophyllum demersum* L.) involves induction of phytochelatins and antioxidant system in response to its accumulation. Chemosphere 65 (6), 1027–1039.
Müller, E., Schüssler, W., Horn, H., Lemmer, H., 2013. Aerobic biodegradation of the sulfonamide antibiotic sulfamethoxazole by activated sludge applied as cosubstrate and sole carbon and nitrogen source. Chemosphere 92 (8), 969–978.
Nimptsch, J., Pflugmacher, S., 2007. Ammonia triggers the promotion of oxidative stress in the aquatic macrophyte *Myriophyllum mattogrossense*. Chemosphere 66 (4), 708–714.
Nomura, Y., Fukahori, S., Fukada, H., Fujiwara, T., 2017. Removal behaviors of sulfamonomethoxine and its degradation intermediates in fresh aquaculture wastewater using zeolite/TiO_2 composites. J. Hazard Mater. 340, 427–434.
Olette, R., Couderchet, M., Biagianti, S., Eullaffroy, P., 2008. Toxicity and removal of pesticides by selected aquatic plants. Chemosphere 70 (8), 1414–1421.
Paddock, S.W., 1999. Confocal microscopy methods and protocols. Cell Biol. Int. 23, 715.
Park, S., Choi, K., 2008. Hazard assessment of commonly used agricultural antibiotics on aquatic ecosystems. Ecotoxicology 17 (6), 526–538.
Quast, C., Pruesse, E., Yilmaz, P., Gerken, J., Schweer, T., Yarza, P., Peplies, J., Glöckner, F.O., 2012. The SILVA ribosomal RNA gene database project: improved data processing and web-based tools. Nucleic Acids Res. 41 (1), 590–596.
Rai, U.N., Sinha, S., Tripathi, R.D., Chandra, P., 1995. Wastewater treatability potential of some aquatic macrophytes: removal of heavy metals. Ecol. Eng. 5 (1), 5–12.
Roy, S., Pellinen, J., Sen, C.K., Hänninen, O., 1994. Benzo(a) anthracene and benzo(a) pyrene exposure in the aquatic plant *Fontinalis antipyretica*: uptake, elimination and the responses of biotransformation and antioxidant enzymes. Chemosphere 29 (6), 1301–1311.
Santos, L.H.M.L.M., Araújo, A.N., Fachini, A., Pena, A., Delerue-Matos, C., Montenegro, M.C.B.S.M., 2010. Ecotoxicological aspects related to the presence of pharmaceuticals in the aquatic environment. J. Hazard Mater. 175 (1–3), 45–95.
Schauss, K., Focks, A., Heuer, H., Kotzerke, A., Schmitt, H., Thiele-Bruhn, S., Smalla, K., Wilke, B.M., Matthies, M., Amelung, W., Klasmeier, J., Schloter, M., 2009. Analysis, fate and effects of the antibiotic sulfadiazine in soil ecosystems. Trac. Trends Anal. Chem. 28 (5), 612–618.
Senta, I., Terzić, S., Ahel, M., 2013. Occurrence and fate of dissolved and particulate antimicrobials in municipal wastewater treatment. Water Res. 47 (2), 705–714.
Su, S.Q., Zhou, Y.M., Qin, J.G., Wang, W., Yao, W.Z., Song, L., 2012. Physiological responses of *Egeria densa* to high ammonium concentration and nitrogen deficiency. Chemosphere 86 (5), 538–545.
Tang, S.Y., Yin, H., Chen, S., Peng, H., Chang, J.J., Liu, Z.H., Dang, Z., 2016. Aerobic degradation of BDE-209 by *Enterococcus casseliflavus*: isolation, identification and cell changes during degradation process. J. Hazard Mater. 308, 335–342.
Thomann, R.V., Mueller, J.A., 1987. Principles of Surface Water Quality Modeling and Control. Harper and Row Publishers, Inc., New York.
Upadhyaya, A., Sankhla, D., Davis, T.D., Sankhla, N., Smith, B.N., 1985. Effect of paclobutrazol on the activities of some enzymes of activated oxygen metabolism and lipid peroxidation in senescing soybean leaves. J. Plant Physiol. 121 (5), 453–461.
Wang, C., Zhang, S., Wang, P.F., Hou, J., Qian, J., Ao, Y.H., Lu, J., Li, L., 2011. Salicylic acid involved in the regulation of nutrient elements uptake and oxidative stress in *Vallisneria natans* (Lour.) Hara under Pb stress. Chemosphere 84 (1), 136–142.
Wang, S.C., 2004. The Adsorption of Polycyclic Aromatic Hydrocarbons to Aquatic Plant (*Naja Gramunea* Del.). Marine Environment and Engineering.
Xian, Q.M., Hu, L.X., Chen, H.C., Chang, Z.Z., Zou, H.X., 2010. Removal of nutrients and veterinary antibiotics from swine wastewater by a constructed macrophyte floating bed system. J. Environ. Manag. 91 (12), 2657–2661.
Xiong, J.Q., Kurade, M.B., Abou-Shanab, R.A.I., Ji, M.K., Choi, J., Kim, J.O., Jeon, B.H., 2016. Biodegradation of carbamazepine using freshwater microalgae *Chlamydomonas mexicana* and *Scenedesmus obliquus* and the determination of its metabolic fate. Bioresour. Technol. 205, 183–190.
Xiong, J.Q., Kurade, M.B., Kim, J.R., Roh, H.S., Jeon, B.H., 2017. Ciprofloxacin toxicity and its co-metabolic removal by a freshwater microalga *Chlamydomonas mexicana*. J. Hazard Mater. 323 (Pt A), 212–219.
Xue, P.Y., Yan, C.Z., 2011. Arsenic accumulation and translocation in the submerged macrophyte *Hydrilla verticillata* (L.f.) Royle. Chemosphere 85 (7), 1176–1181.
Yadav, T.C., Khardenavis, A.A., Kapley, A., 2014. Shifts in microbial community in response to dissolved oxygen levels in activated sludge. Bioresour. Technol. 165, 257–264.
Yan, C., Yang, Y., Zhou, J., Liu, M., Nie, M., Shi, H., Gu, L., 2013. Antibiotics in the surface water of the Yangtze Estuary: occurrence, distribution and risk assessment. Environ. Pollut. 175, 22–29.

Yan, J., Lei, M., Zhu, L., Anjum, M.N., Zou, J., Tang, H., 2011. Degradation of sulfamonomethoxine with Fe_3O_4 magnetic nanoparticles as heterogeneous activator of persulfate. J. Hazard Mater. 186 (2–3), 1398–1404.
Yan, Z.S., Jiang, H.L., Cai, H.Y., Zhou, Y.L., Krumholz, L.R., 2015. Complex interactions between the macrophyte *Acorus Calamus* and microbial fuel dells during Pyrene and Benzo[a]Pyrene degradation in sediments. Sci. Rep. 5 (1), 19017.
Yang, C.W., Hsiao, W.C., Chang, B.V., 2016. Biodegradation of sulfonamide antibiotics in sludge. Chemosphere 150, 559–565.
Yang, S.F., Lin, C.F., Wu, C.J., Ng, K.K., Lin, A.Y.C., Hong, P.K.A., 2012. Fate of sulfonamide antibiotics in contact with activated sludge-sorption and biodegradation. Water Res. 46 (4), 1301–1308.
Yin, L.Y., Huang, J.Q., Li, D.H., Liu, Y.D., 2005. Microcystin-RR uptake and its effects on the growth of submerged macrophyte *Vallisneria natans* (Lour.) Hara. Environ. Toxicol. 20 (3), 308–313.
Zhang, T., Ren, H.F., Liu, Y., Zhu, B.L., Liu, Z.P., 2010. A novel degradation pathway of chloroaniline in *Diaphorobacter* sp. PCA039 entails initial hydroxylation. World J. Microbiol. Biotechnol. 26 (4), 665–673.
Zhang, W.W., Wen, Y.Y., Niu, Z.L., Yin, K., Xu, D.X., Chen, L.X., 2012. Isolation and characterization of sulfonamide-degrading bacteria *Escherichia* sp. HS21 and *Acinetobacter* sp. HS51. World J. Microbiol. Biotechnol. 28 (2), 447–452.
Zhang, Y., Yan, Z.S., Wu, H.F., Jiang, H.L., Hao, Z., 2018. Remedial function of submersed macrophyte *Vallisneria natans* to PAHs-contaminated sediments. J. Lake Sci. 30 (4), 1012–1018.
Zhao, L., Ji, Y., Sun, P.Z., Li, R.Y., Xiang, F., Wang, H.Y., Ruiz-Martinez, J., Yang, Y.K., 2018. Effects of individual and complex ciprofloxacin, fullerene C_{60}, and ZnO nanoparticles on sludge digestion: methane production, metabolism, and microbial community. Bioresour. Technol. 267, 46–53.
Zhu, Z.J., Yuan, H.Z., Wei, Y., Li, P.S., Zhang, P.H., Xie, D., 2016a. Effects of ammonia nitrogen and sediment nutrient on growth of the submerged plant *Vallisneria natans*. Clean. - Soil, Air, Water 43 (12), 1653–1659.
Zhu, Z.J., Song, S.Y., Li, P.S., Jeelani, N., Wang, P.H., Yuan, H.Z., Zhang, J.H., An, S.Q., Leng, X., 2016b. Growth and physiological responses of submerged plant *Vallisneria natans* to water column ammonia nitrogen and sediment copper. Peerj 4 (1), 1953.
Zhuang, H.F., Han, H., Jia, S.Y., Hou, B.L., Zhao, Q., 2014. Advanced treatment of biologically pretreated coal gasification wastewater by a novel integration of heterogeneous catalytic ozonation and biological process. Bioresour. Technol. 166, 592–595.